Ecological Modelling 470 (2022) 110016

Contents lists available at ScienceDirect

Ecological Modelling

journal homepage: www.elsevier.com/locate/ecolmodel

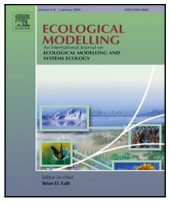

Analysis of simulated trap counts arising from correlated and biased random walks

Omar Alqubori [a,*], Sergei Petrovskii [b]

[a] Faculty of Science, University of Jeddah, Saudi Arabia
[b] School of Mathematics and Actuarial Science, University of Leicester, University Rd, Leicester, United Kingdom

ARTICLE INFO

Keywords:
Baited trap
Trap counts
Pattern formation
Individual-based modelling

ABSTRACT

Traps are routinely used in insect ecology, conservation, and pest control, but the understanding of trap counts remains limited. A well developed theory only exists for non-baited traps (e.g. pitfall traps) and the simplest animal movement modes, such as Brownian motion, but not for more complex or realistic situations. In particular, important questions as to how the trap counts may differ in case of a baited trap and what its effect can be on the population distribution in the domain where the trap is installed are largely open. In order to bridge this gap in our knowledge, here we use straightforward yet powerful simulation framework of individual-based modelling. A baited trap has a strong effect on the animal movement pattern changing it from the Correlated Random Walk to the Biased Random Walk. This, in turn, is shown to have a dramatic effect on the trap counts. We show that a baited trap can introduce strong heterogeneity into the spatial population distribution, hence resulting in spatiotemporal pattern formation. We also consider a system of multiple traps and show that the trap efficiency can decrease if the traps are installed close to each other.

1. Introduction

Evaluation of population abundance is a task frequently arising in ecology and agro-ecology (Seber, 1982), for instance in the context of nature conservation or pest control (Binns et al., 2000; Pedigo, 1999). Depending on the species traits, the overall goal of a study and the available resources, there is a variety of means to do it, e.g. by direct counting of the individuals (McDonald and Hodgson, 2021). One of the common approaches, in particular for small arthropods such as insects and gastropods, is the use of the traps (Pedigo, 1999; Baars, 1979; Epsky et al., 2008; Jonason et al., 2014; Raworth and Choi, 2001). One or several traps are installed in a study area (to which we will refer as a field); after a certain time interval, their content is checked and the number of individuals of a given species is counted. Based on the trap count, a conclusion is then made about the corresponding population abundance in the field. Often the traps remain in the field over a considerable stretch of time, so that the above procedure is repeated several or many times, hence resulting in a series of trap counts.

Straightforward as it may seem at the first sight, interpretation of the trap count(s) often poses a significant challenge (Jonason et al., 2014; Engel et al., 2017; Boetzl et al., 2018; Ahmed and Petrovskii, 2019). In fact, there is only one conclusion that can be made unambiguously: if the trap count contains individuals of a given species, then this species is indeed present in the field. However, the opposite is not true: the absence of individuals of a given species in the trap count does not necessarily mean that the species is absent from the field. Because animal movement often can be regarded as a random process (Codling et al., 2008; Turchin, 1998), their absence in the trap count may as well happen simply by chance, e.g. if the population density is low and the time of trap exposure was not long enough. It can also result from an inefficient or inadequate trap design that does not fully take into account species traits.

Thus, even the interpretation of presence/absence data may bring some difficulties, and the estimation of the population density based on trap counts is a much more difficult problem (Petrovskii et al., 2014). In fact, due to the inherent randomness of the processes resulting in trapping, to work out a sensible estimate based on a single trap count is impossible. In the case where several trap counts are available, the estimation in principle becomes possible but strongly depends on the trap type or design (Brown and Matthews, 2016). A consistent theory only exists in the case of 'passive' non-baited traps[1] (Pedigo, 1999; Ahmed and Petrovskii, 2019; Bearup et al., 2016; Petrovskii et al., 2012), i.e. in the case where the presence of the trap does not change the animals movement pattern until they fall into the trap.

* Corresponding author.
E-mail addresses: Ommohamad3@uj.edu.sa (O. Alqubori), Sp237@leicester.ac.uk (S. Petrovskii).

[1] For instance, for ground-walking insects, such non-baited trap can be just a hole in the ground to which they occasionally fall — the so called "pitfall traps"

https://doi.org/10.1016/j.ecolmodel.2022.110016
Received 20 September 2021; Received in revised form 2 May 2022; Accepted 5 May 2022
Available online 24 May 2022

An alternative trap type is refereed to as 'active' or baited traps. The general idea of a baited trap is that they contain a bait or a lure: something that animals can perceive from a considerable distance and that attracts them to its source, i.e. to the trap. The nature of the lure depends on the species traits; for instance, there are pheromone-baited, light-baited and colour-baited traps (Epsky et al., 2008). Whichever is the case, the generic effect of a baited trap is to change the inherent animal movement pattern by making their movement towards the trap more likely. Baited traps are frequently used due to their proven efficiency in catching animals, not only for monitoring purposes but also for pest control as they are capable to catch individuals of a harmful species in large numbers; the corresponding control strategy being known as "mass trapping" (El-Sayed et al., 2006). In spite of that, somewhat paradoxically, any consistent theory allowing for the baited trap counts analysis is largely missing (but see Byers et al., 1989; Byers, 1999). Their interpretation is usually relative rather than absolute (i.e. a larger trap count is assumed to correspond to a larger population density) and is often based on heuristic, semi-intuitive concepts and quantities such as, for instance, the attraction radius and the trap catchment area (also known as the effective sampling area, e.g. Turchin and Odendaal, 1996). Perhaps even more importantly, the effect of the baited traps on the distribution of the monitored population is hardly known at all. Meanwhile, such effect can be significant, as even non-baited traps are known to disturb the animal distribution considerably (Petrovskii et al., 2012, 2014).

We mention here that good understanding of the effect of baited traps on monitored species is also needed in a broader framework of ecosystem-scale processes. Indeed, animal movement, e.g. in the context of animal dispersal, is regarded as a major factor that brings different aspects of ecosystem's functioning together (Clobert et al., 2001; Bullock et al., 2002; Turchin, 2013). Disruption or alternation of natural animal movement patterns can cause significant disruption in the ecosystem level processes and functions. Therefore, mathematical models of the whole-system processes, in particular in agricultural systems, must take the effect of traps on the population distribution of targeted species into account (Guichard et al., 2012; Tonnanga et al., 2017; Yamanaka et al., 2003).

In this paper, we endeavour to partially bridge this gap in our knowledge by looking into the effect of baited traps on the spatial distribution of an animal population (to which we for convenience will refer as insects) and the variety of situations and factors affecting the trap counts. The paper is organised as follows. In Section 2, we describe our mathematical model and the details of simulation procedure. In Section 3, we present the simulation results obtained in the case of a single trap, in particular to reveal the effect of persistence in the individual animal movement, the strength of attraction by a baited trap, the effect of the trap design and the domain shape. In Section 4, we extend our investigation onto the case where a few traps (e.g. two or three) are installed. In particular, we will show that, depending on the distance between the traps, they can start interacting and that can have a significant effect both on the trap counts and the spatial population distribution. In Section 5, we discuss our main findings and their implications.

2. Mathematical model

2.1. Individual-based vs mean-field models

There exists a variety of modelling techniques to simulate the evolution of population distribution in the presence of trap(s). They can roughly be sorted into two qualitatively different types such as individual-based models (IBM) and mean-field (MF) models. The latter describes the population as a whole in terms of the population density; usually, models of this type consist of either partial differential equations (e.g. the diffusion equation (Bearup et al., 2015, 2016) or the telegrapher equation (Alharbi and Petrovskii, 2018; Tilles and Petrovskii, 2019) or integral equations (Petrovskii et al., 2014)). The former describes the movement of every individual in a given population (Jopp and Reuter, 2005); this information can be summarised to reveal the corresponding changes in the population distribution (Petrovskii et al., 2022).

Each of these approaches has its strengths and weaknesses. The power of the IBM is that it allows to account for details of individual behaviour at the 'microscale' related to a single individual. Also, it is usually straightforward to implement, which makes it accessible to a broad variety of researchers with different background. Its main drawback is that it is essentially simulation-based. Every particular simulation run uses a particular parameter set and hence by itself gives only very little information about the system properties more generally; in order to obtain such information (e.g. the structure of the parameter space), one has to perform many simulation runs for different parameter values, which can be expensive and time-consuming.

The main power of the MF models is that they can, in principle, be solved or analysed analytically, at least sometimes, which can provide a general and reliable information about the system properties as a whole. In practice, however, a comprehensive mathematical analysis is rarely possible. Even for the standard model such as the diffusion equation, its explicit solution is only available for spatial domains with a simple, idealised geometry. Any more realistic problem has to be solved numerically, often using elaborate numerical methods, so that, in practical terms, there is little difference between the IBM and the MF models as simulations have to be used anyway. Moreover, for MF models more complicated (and, arguably, more realistic) than the diffusion equation, there may arise more fundamental problems related to the adequate choice of the boundary conditions. For instance, in the case of the telegrapher equation, which is the MF counterpart for the correlated individual random walk, the solution is only positively defined only for a specific choice of the boundary and/or initial conditions (Alharbi and Petrovskii, 2018; Tilles and Petrovskii, 2019).

Given the above, in this paper we use the IBM approach as it seems to be better fit for the goals of the study. Details of our model are described in the next section.

2.2. The baseline IBM model

In its movement, an animal usually follows a curvilinear path. However, curves are difficult to analyse. A common approach (Kareiva and Shigesada, 1983; Jopp and Reuter, 2005; Edelhoff et al., 2016) approximates the continuous time by a discrete time with a certain time step Δt, i.e. $t_{i+1} = t_i + \Delta t$ where $i = 0, 1, 2, \dots$. Generally speaking, Δt can also be a function of i; here we consider it constant. In terms of empirical studies on animal movement, moments t_i correspond to the moments when the animal position is recorded. Correspondingly,

$$\mathbf{r}_i = \mathbf{r}(t_i), \quad i = 0, 1, 2, \dots , \tag{1}$$

where $\mathbf{r}_i = (x_i, y_i)$ is the animal's position at time t_i (hence considering the movement in a 2D space, e.g. on the surface of the ground), $\mathbf{r}_0$ being its initial position. Correspondingly, a given continuous curve (movement path) is replaced with a broken line.

A given broken line is fully determined by the corresponding sequence of step sizes $\{l_i\}$, where l_i is the length of the link connecting two subsequent positions, $l_i = |\Delta \mathbf{r}_i| = |\mathbf{r}_{i+1} - \mathbf{r}_i|$, and the sequence of the turning angles $\{\theta_i\}$ between the two adjacent links. Since $\Delta \mathbf{r}_i = (\Delta x_i, \Delta y_i)$, obviously

$$l_i^2 = \Delta x_i^2 + \Delta y_i^2 \quad \text{and} \quad \theta_i = \arctan\left(\frac{\Delta y_i}{\Delta x_i}\right). \tag{2}$$

Note that Eqs. (2) effectively describe the change in the path description between the Cartesian and polar coordinates.

If animal movement can be regarded as random, which is often the case (but see Turchin (1998) for a discussion of the "bugbear

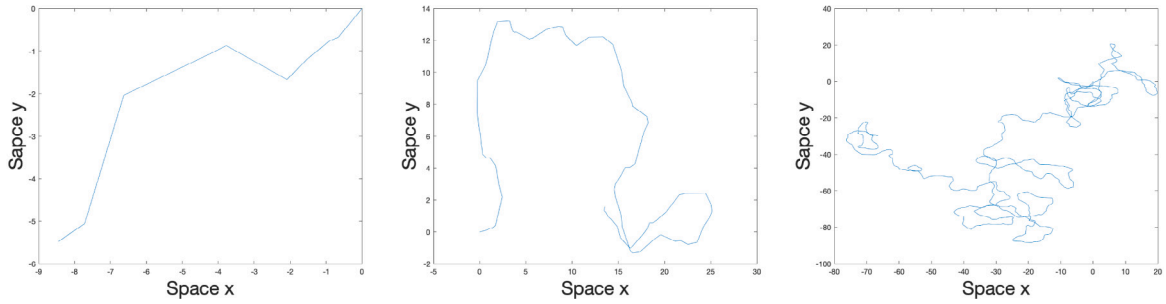

Fig. 1. Animal's movement path simulated using the CRW with $p_0 = 0.5$ over a time interval of different duration: from left to right, 10, 100, and 1000 time steps. The initial animal's position is at the origin.

of randomness"), both l_i and θ_i become random values defined by their probability distribution functions, say, $S(l)$ and $P(\theta)$, respectively. Different movement patterns correspond to S and P with different properties and vice versa. For instance, the rate of decay in S at large l is a property that differentiates between Brownian and non-Brownian random walks. While the exponential or faster-than-exponential rates are characteristic for the Brownian motion (BM), a slower rate (e.g. a power law with a sufficiently small exponent) correspond to a Levy walk (Klafter et al., 1996; Viswanathan et al., 1996, 2011). In this study, we mostly focus on the effect of the turning angle (see below) and hence stick to the case where $S(l)$ decays sufficiently fast. Specifically, we consider S to be the half-normal distribution:

$$S(l;\delta) = \frac{\sqrt{2}}{\delta\sqrt{\pi}} \exp\left(-\frac{l^2}{2\delta^2}\right), \quad l \geq 0, \tag{3}$$

where δ is the distribution parameter.

The probability distribution of the turning angle is a factor that help to further differentiate between different random walk types. In case of BM, the angle is distributed uniformly over the circle:

$$P(\theta) = \frac{1}{2\pi}. \tag{4}$$

In case of animal movement, especially if considered at a sufficiently small time scale (i.e. for a sufficiently small Δt), this is not realistic as it implies frequent abrupt turns and hence cannot approximate a smooth movement path. A more realistic alternative to BM is the Correlated Random Walk (CRW) (Kareiva and Shigesada, 1983) where the turning angle distribution has the maximum at $\theta = 0$ and the standard deviation is significantly smaller than π, so that small turning angles are more likely than large ones. Thus, the CRW takes into account the correlation between the turning angle in any two consequent steps.

For simulations, we use the truncated normal distribution:

$$P(\theta) = \frac{C}{p_0\sqrt{2\pi}} \exp\left(-\frac{\theta^2}{2p_0^2}\right), \quad -\pi \leqslant \theta \leqslant \pi, \tag{5}$$

where C is the normalising coefficient to ensure that the total probability is 1 and p_0 is a parameter called persistence. The smaller p_0, the more likely the movement direction in the next step along the path is close to the direction in the previous step and hence the more directed the movement is.

Note that both BM and the CRW assume that the space is isotropic, i.e. there is no any particular direction that would be favoured by the animals in their movement. Although this assumption is feasible in many cases, it is hardly realistic in the presence of a baited trap: indeed, the main idea of the baited trap is to ensure that the movement towards the trap is more likely than in any other direction. In order to account for this movement type, we consider the Biased Random Walk (BRW) (Codling et al., 2008) where the turning angle is distributed as follows:

$$P(\theta,\kappa) = \frac{C}{p_0\sqrt{2\pi}} \exp\left(-\frac{(\theta-\kappa)^2}{2p_0^2}\right) \quad -\pi \leqslant \theta \leqslant \pi, \tag{6}$$

where κ is the bearing of the baited trap taken at the current animal's position (x_i, y_i). Let (x_{trap}, y_{trap}) be the trap position, then, obviously, $\kappa = \arctan\left(\frac{y_i - y_{trap}}{x_i - x_{trap}}\right) \pm \pi$ when $x_i < x_{trap}$; and $\kappa = \arctan\left(\frac{y_i - y_{trap}}{x_i - x_{trap}}\right)$ when $x_i > x_{trap}$.

Using distributions S and P, the animal's movement path can be generated for each of the movement type; examples are shown in Figs. 1–2. We readily observe that the complexity of the movement path depends on the timescale: a longer time span generates a path of a more complicated (less regular) shape.

In the below, we consider the simultaneous movement of N identical non-interacting animals, so that the movement path of each of them is generated in the same way. We consider animal movement in a computational domain of a square shape, i.e. $-L \leq x_i^k \leq L$ and $-L \leq y_i^k \leq L$ $(k = 1, 2, \ldots, N,\ i = 0, 1, 2, \ldots)$, L being the domain size. For the initial condition, we use a random distribution: for each animal, both x_0^k and y_0^k are random numbers uniformly distributed on $(-L, L)$. The domain is closed, so that animals cannot leave it through the external boundary; when an animal hits the boundary in its random movement, it is returned back to the domain.

2.3. Modelling trap counts

In simulations, a trap is defined as a sub-domain of a certain shape with a characteristic size much smaller than the size of the whole computational domain. As soon as animal in its movement hits the trap boundary, it is regarded as 'trapped': its movement path terminates, the animal is removed from the system and the trap count (the number of caught animals) increases by one.

Consider a circular trap of radius R with the coordinates of its centre as (x_{trap}, y_{trap}). The mathematical conditions describing the capture of the kth animal at moment t_j are as follows:

$$\left(x_i^k - x_{trap}\right)^2 + \left(y_i^k - y_{trap}\right)^2 > R^2, \quad i = 0, 1, \ldots, j-1, \tag{7}$$

$$\left(x_j^k - x_{trap}\right)^2 + \left(y_j^k - y_{trap}\right)^2 < R^2. \tag{8}$$

Obviously, at the same moment of (discrete) time, more than one animal can be caught. Let $M(t_j)$ be the 'daily count', i.e. the number of animals caught at moment t_j and let $T(t_{j-1})$ be the total (cumulative) number of animals caught over the preceding time, then $T(t_j)$ is calculated as

$$T(t_j) = T(t_{j-1}) + M(t_j) = \sum_{k=1}^{j} M(t_k). \tag{9}$$

Thus, the cumulative trap count T is an increasing (more generally, non-decreasing) function of time.

2.4. Mean-field approach: Diffusion equation

In case the number of insects in the area is sufficiently large, their distribution can be described by the population density. While the

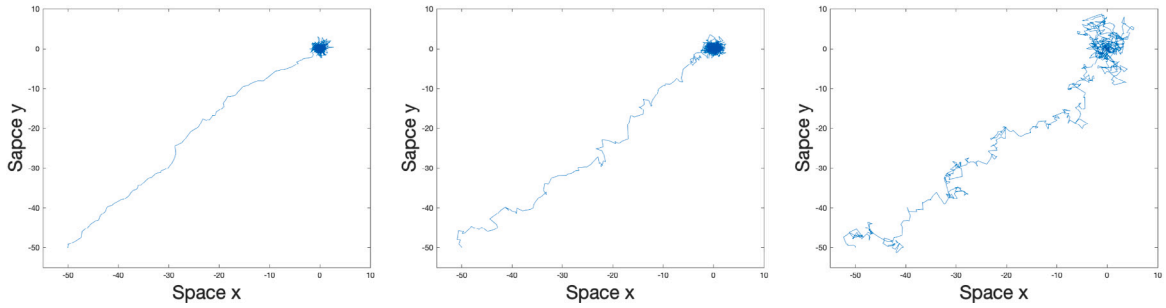

Fig. 2. Animal's movement path simulated using the BRW over the time interval of 1000 steps for different persistence values: left to right, $p_0 = 0.5, 1, 2$. The baited (attracting) trap is located at the origin, $(x_{trap}, y_{trap}) = (0, 0)$, the initial animal's position is $(-50, -50)$.

movement of an individual animal is often almost entirely random (but see Turchin (1998), Pyke (2015)), changes in the population density are usually more regular and more predictable. In models, the population density is a solution of a mean-field equation. As each of these two modelling approaches has its own drawbacks (see Section 2.1), they work best when used in combination. In particular, in modelling trap counts, by considering a relevant mean-field solution against the IBM simulations, one can reveal the pattern and estimate the underlying population density (Petrovskii et al., 2012, 2014).

As we have discussed it above, even in the baseline case of diffusion equation (respectively, for individual insects performing BM), an explicit exact solution is only available for a very special, unrealistic choice of system's geometry. However, for a more general and more realistic case, such as a circular trap installed in a domain of an arbitrary shape (but sufficiently far away from the domain boundary), the following approximate expression was shown to provide a sufficiently accurate description of the cumulative trap counts (Petrovskii et al., 2012):

$$S_{MF} \approx \frac{2Up}{\sqrt{\pi}}\sqrt{Dt}\left(1 + \frac{\alpha\pi}{p}\sqrt{Dt}\right), \tag{10}$$

where p is the trap perimeter ($p = 2\pi R$ for a circular trap), U is the initial population density (assuming that initially the population is distributed uniformly) and α is a numerical coefficient on the order of one. The diffusion coefficient D can be related to the properties of individual animal movement as

$$D \approx \frac{\delta^2}{2\Delta t}, \tag{11}$$

where δ^2 is the variance of the step size distribution.

We emphasise that Eq. (10) was obtained in the case of diffusive movement and it is not necessary valid for a more general case of the CRW. However, since the CRW is known to converge to BM after a sufficiently large number of steps (depending on the persistence), one can expect that Eq. (10) may, on a certain time scale, provide a reasonably good description of the trap counts arising in the population where individuals perform the CRW. That will be investigated below.

3. Simulation results: trap counts by a single trap

In our IBM simulations, unless stated differently we consider the insect population consisting of $N = 10^4$ individuals moving in a square $L \times L$ domain centered at the origin, with size $L = 100$ (except for Section 3.2 where $L = 200$). A circular trap of a certain radius R is placed at the origin, i.e. at the centre of the domain. The distribution of step size is always considered as in Eq. (3) with $\delta = 1$, our goal is to reveal how the cumulative trap counts (see Eq. (9)) depend on the distribution of turning angle, i.e. on the movement type; see Eqs. (5) and (6).

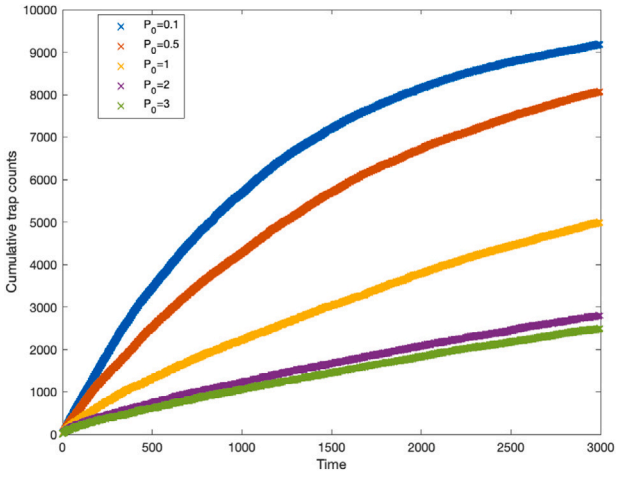

Fig. 3. Cumulative trap count vs time obtained for different values of p_0 as shown in the figure legend. Here, as well as in all similar figures below, time is shown as a number of time steps; see Section 2.2 for details. The trap is non-baited, so insects perform the CRW. The trap radius is $R = 5$, the domain size is $(-50, 50) \times (-50, 50)$ (i.e. $L = 100$) and the total insect population is 10^4.

3.1. Effect of persistence

In this section, insect movements are assumed to perform the CRW so that their movement is described by Eqs. (3) and (5). Our goal here is to reveal how the trap count dependence on time may be altered by the movement persistence, as quantified by parameter p_0.

Fig. 3 shows the cumulative trap counts over time obtained for different values of p_0. We readily observe that the trap efficiency (the total number of insects caught over a given interval) strongly depends on the movement type. In case of a low persistence (large values of p_0, see the green and purple curves), i.e. when the distribution of turning angle is almost uniform over the circle and hence animal movement is approximately Brownian, the trap efficiency is much smaller than in case of a high persistence. The highest efficiency is achieved when $p_0 = 0.1$ when an individual insect path becomes close to a straight line (cf. Fig. 1, left).

We also observe that in all cases the graph of the trap count dependence on time is a concave curve: apparently, the trap efficiency decreases with time. The reason for this can be understood if one looks into the spatial distribution of animals around the trap. Snapshots of such distribution obtained at a certain moment of time for two values of p_0 are shown in Fig. 4. The presence of trap introduces heterogeneity into the population distribution, so that the insect density is smaller in a small vicinity of the trap, this effect of the trap being more distinct for low persistence. A heuristic explanation of this is that, since animal displacement in case of a low-persistent movement (effectively, Brownian motion) is slow, the animals caught by the trap

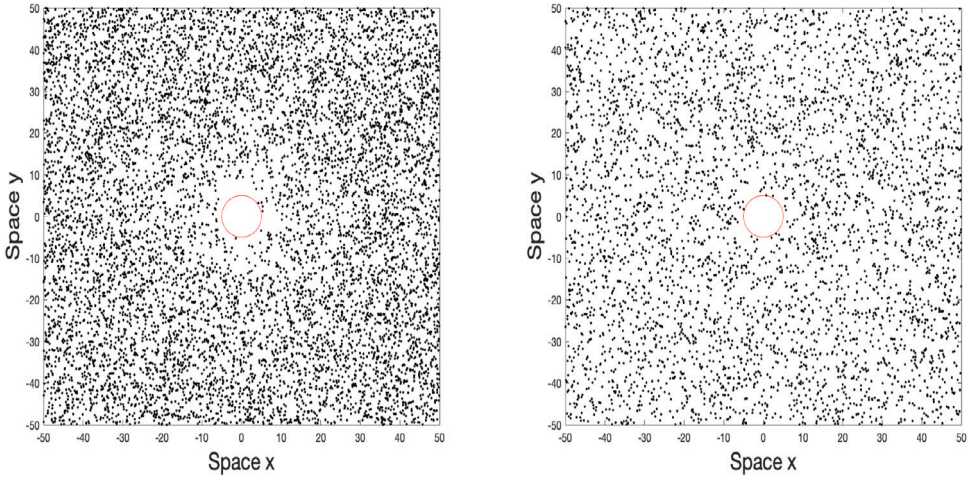

Fig. 4. Snapshots of the insects spatial distribution over the simulation domain obtained after 1000 time steps. Insects perform the CRW with (left) $p_0 = 2$ (low persistence) and (right) $p_0 = 0.1$ (high persistence). Other parameters as in Fig. 3.

in its immediate vicinity are not compensated sufficiently fast by the arrival of new ones from a larger distance.

3.2. Is a small baited trap equivalent to a large non-baited trap?

In some studies, attempts were made to interpret a baited trap as a non-baited trap of a much larger size, i.e. with the radius equal to the attraction radius of the 'catchment area' of the baited trap, cf. (Byers et al., 1989; Byers, 1999). Such catchment area can be thought of as a (large) circle with the radius determined by the animals perception distance, that is, in the case of a light-baited trap, the maximum distance at which the intensity of light is still strong enough to be perceived by the insects and hence to alter their movement behaviour. In this section, our goal is to check this hypothesis.

A baited trap of radius $R_b = 5$ is installed at the centre of the field. The effect of bait (e.g. the light intensity for light-baited traps) decreases with the distance from the trap, eventually falling to a very small value, so that the insects located at sufficiently large distance do not perceive it and hence move as if there is no trap, e.g. performing the CRW. We therefore introduce the attraction radius, say R_{Att}, so that the kth insect performs the CRW at the moment t_i if

$$(x_i^k - x_{trap})^2 + (y_i^k - y_{trap})^2 > R_{Att}^2, \tag{12}$$

but changes its movement pattern to the BRW if

$$(x_i^k - x_{trap})^2 + (y_i^k - y_{trap})^2 < R_{Att}^2. \tag{13}$$

Thus, when insects enter the attraction area, they move towards the trap in a much more directed manner. Since insects performing the BRW will almost never go away from the baited trap, the attraction area plays the role of the catchment area and its radius plays the role similar to that of the radius of a non-baited trap.

Fig. 5 compares the cumulative trap count (see Eq. (9)) obtained for the baited trap with that obtained for the large 'equivalent' non-baited trap with radius $R = R_{ATT}$ (for which we use a hypothetical value $R_{ATT} = 35$). Note that, since the radius of the non-baited trap is rather large, in order to exclude the effect of domain boundaries, here we consider a larger domain with $L = 200$, that is $-100 \le x, y \le 100$. Since trap counts depend on the population density, in order to make the obtained trap counts comparable with other results in this paper, we also consider a larger population size, namely $N = 4 \cdot 10^4$. The blue curve in Fig. 5 shows the cumulative trap count obtained for the baited trap and the red curve shows the cumulative trap count obtained for the large non-baited trap. We observe that the two traps are not equivalent, as the curves have different shapes (concave for the non-baited trap and sigmoid for the baited trap). In particular, at a small

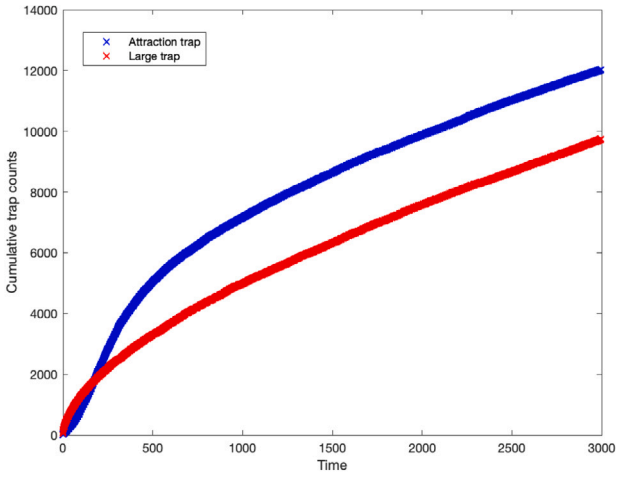

Fig. 5. Cumulative trap counts vs time (shown as the number of time steps) calculated for a baited trap (blue curve) with $R_b = 5$ and the attraction radius of $R_{ATT} = 35$ and the 'equivalent' large non-baited trap (red curve) of radius $R = R_{ATT} = 35$. In both cases, the persistence parameter is $p_0 = 2$. The domain size is $L = 200$ and the initial insect population is $N = 4 \cdot 10^4$.

time (approximately over the first 250 time steps) the cumulative trap count for the baited trap grows at an accelerating rate (as this part of the curve is convex). Thus, in real-life applications, interpreting it as trap counts by a non-baited trap can give a wrong, misleading message as it can be regarded as a sign that the population density in the domain (field) is increasing and hence may lead to unjustified decisions about pest control measures.

Interestingly, the relative efficiency of the traps changes with time. At a small time, the non-baited trap appears to be more efficient, as its cumulative trap count is larger than that of the baited trap; however, the situation changes to the opposite at a large time.

In order to provide a more detailed comparison between the two traps, Fig. 6 shows the corresponding simulated insect spatial distribution. We readily observe that in the case of the large non-baited trap the distribution is qualitatively the same as in Section 3.1 (see also Petrovskii et al., 2012), i.e. the population density in the immediate vicinity of the trap falls to a small value. Interestingly, for the baited trap, it is qualitatively different: in this case, the minimum population density is reached at an intermediate distance from the trap while close to the trap the density is large (see Fig. 6, right).

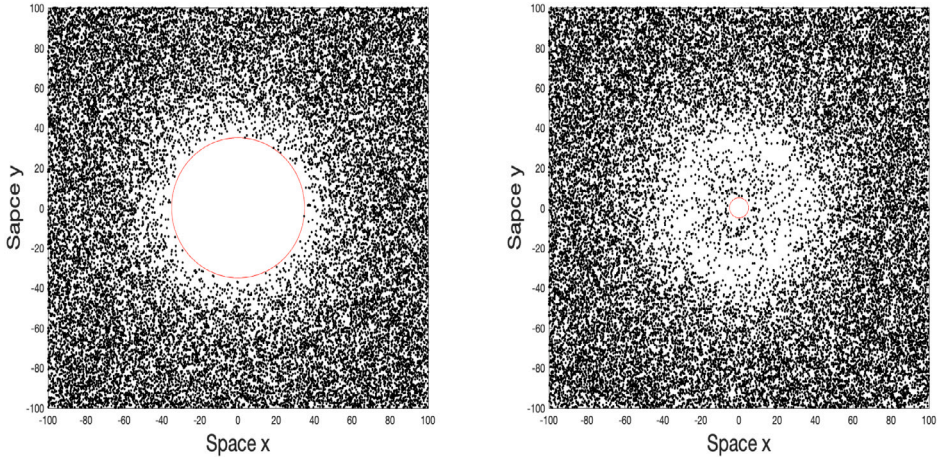

Fig. 6. Snapshots of the spatial population distribution obtained after 3000 time steps in case of (left) a large non-baited trap of radius $R = R_{ATT} = 35$ and (right) a small baited trap of radius $R_b = 5$. Other parameters are the same as in Fig. 5.

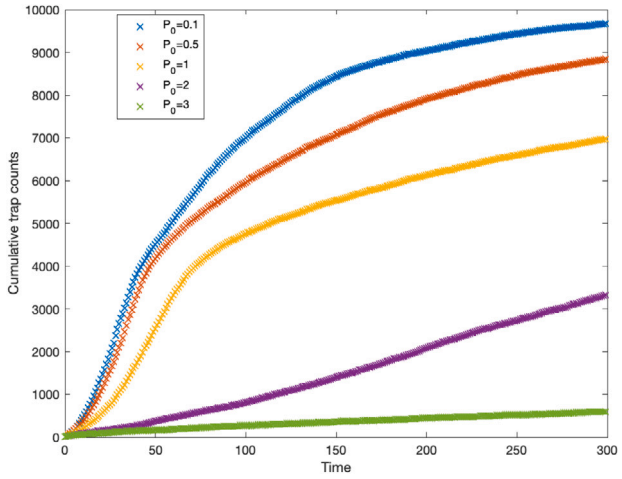

Fig. 7. Cumulative trap count for the baited trap obtained for different values of p_0. The radius of the trap is $R_b = 5$; the attraction radius is $R_{Att} = 35$. Here the domain size is $L = 50$ and the total insect population is $N = 10^4$.

As it was shown in Section 3.1 in the case of the CRW, the trap efficiency depends significantly on the movement persistence, i.e. on parameter p_0. The question therefore arise whether similar effect of the movement persistence takes place in the case of the BRW. In order to make an insight into this, we performed simulations with the baited trap for different values of p_0 in Eq. (6). The results are shown in Fig. 7. We observe that a decrease in p_0 not only leads to a significant increase in the cumulative trap count (hence increasing the trap efficiency) but has a somewhat more subtle effect by altering the shape of the curve: the convex part of the curve shrinks towards small time and the transition between the convex and concave parts becomes more abrupt.

3.3. Baited trap may lead to formation of transient patterns

In this section, we will have a more systematic look into the effect of the attraction produced by a baited trap. We first consider a trap of radius $R_b = 5$ installed at the origin of a square domain $[-L, L]\times[-L, L]$ with $L = 50$. We assume that the attraction radius is large, $R_{ATT} > L$, so that insects perform the BRW across the whole domain.

The results are shown in Fig. 8. We observe that, in case of a large p_0, the spatial population distribution is similar to the case of a non-baited trap (i.e. where insects perform the CRW) apart from the emergence of an area along the domain border with a somewhat lower population density (Fig. 8, left). However, in case of a sufficiently small value of p_0 (high persistence of the individual movement), the trap introduces a distinct heterogeneity into the population distribution: a cross-shaped spatial pattern emerges. The pattern is transient: the cross-shaped distribution is eventually shrinking with time (not shown here), as insects continue moving towards the trap.

We hypothesise that the curious shape of the population distribution emerging in case of a small p_0 is an effect of the domain shape. Indeed, it is readily seen that the minimum distance from the trap to the domain border (i.e. along the coordinate axes) is about 1.4 times shorter than the maximum distance (i.e. to the domain corners). Correspondingly, after a given time interval, the insects that started their approach to the trap from locations at (or close to) $(\pm L, 0)$ and $(0, \pm L)$ will be significantly close to the trap than the insects that started from the corners.

In order to check this hypothesis, we repeat the same simulations as above but now considering the domain of a circular shape with the radius $R_D = L = 50$. Since the circular domain of this size has the area somewhat smaller than the square one, in order to maintain the same initial population density we use a smaller population size, namely $N = 8 \cdot 10^3$.

The results are shown in Fig. 9. We readily observe that, in this case, the population distribution keeps the circular symmetry for any value of p_0, no pattern emerges.

In conclusion of this section, Fig. 10 shows the cumulative trap count obtained for the two fields. We observe that, in spite of the pattern formation in the case of the square field, there is no difference in the shape of the curves; in fact, they are practically the same until approximately $t \approx 500$. At a later time, the efficiency of the trap in the square field appears to be slightly higher, e.g. by time $t = 1000$ it catches a somewhat larger number of insects compared to its counterpart in the circular field. That, however, can be the effect of saturation in the trap count curve: if considered as the percentage of the total initial population size, this number is higher in the circular field than in the square one, 95% against 80%, respectively.

3.4. Effect of a mixed-type trap

We now consider trap counts by a trap of a different design. Namely, we assume that the light-baited trap is shadowed on one side. It can still catch insects that cross the trap boundary but it only has an attractive power on one side, by not on the other side. Thus, such 'hybrid' trap is effectively a combination of a baited trap if approached from one side – from the positive direction of coordinate y (or, in polar coordinates, from the range of polar angle $0 \le \phi \le \pi$) – and non-baited trap if

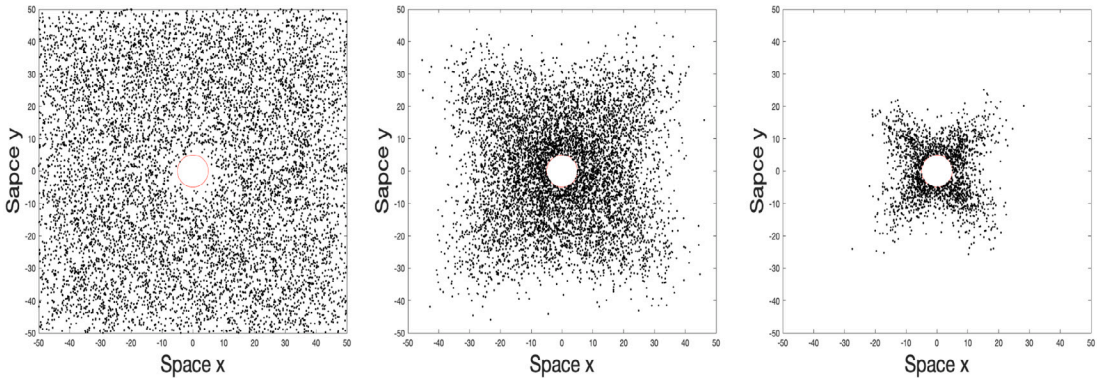

Fig. 8. Snapshots of the population distribution in a square domain obtained at $t = 1000$ in the case of a baited trap with a different strength of the bias in insect movement, i.e. different values of p_0. Left to right: $p_0 = 3, 1.5$ and 1, respectively. The trap radius $R_b = 5$ and the total insects population is $N = 10^4$.

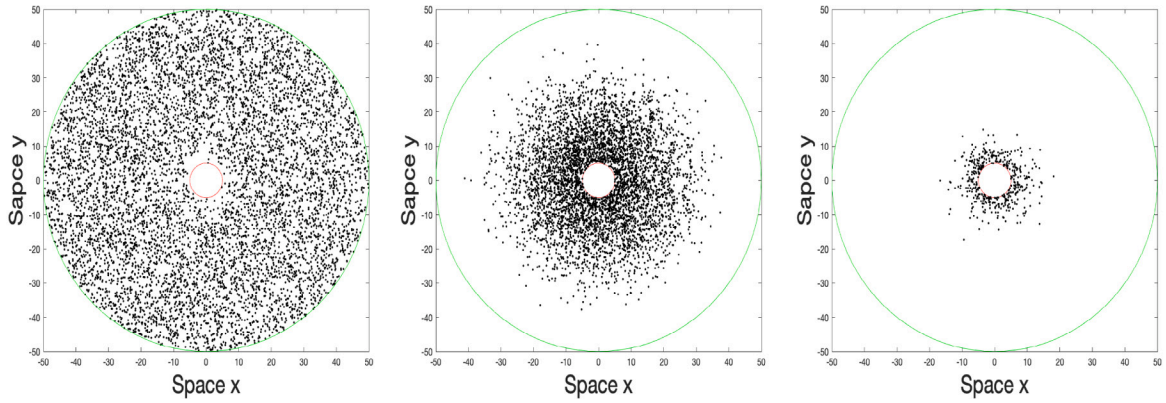

Fig. 9. Snapshots of the population distribution obtained at $t = 1000$ in the case of a baited trap installed in a circular field. Left to right: $p_0 = 3, 1.5$ and 1, respectively. The trap radius $R_b = 5$ and the total insects population is $N = 8 \cdot 10^3$.

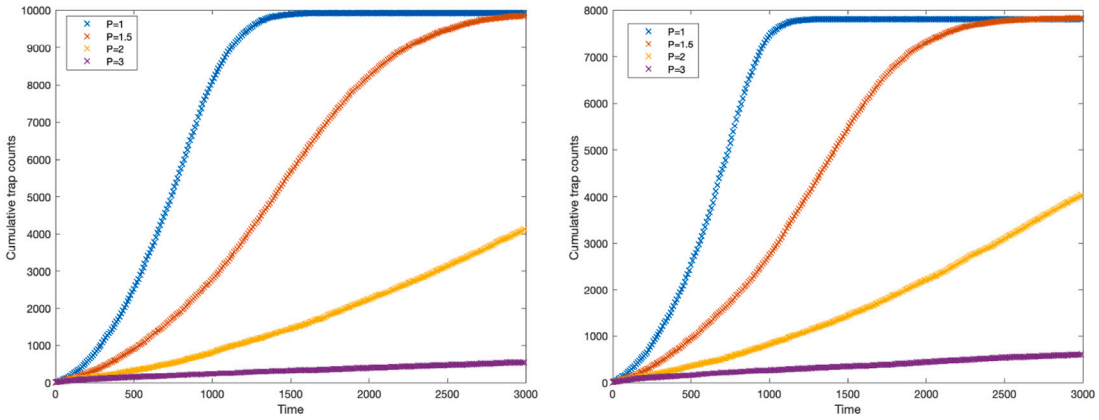

Fig. 10. Cumulative trap count by a baited trap vs time in a square and circular domain, left and right, respectively, obtained for different value of persistence parameter p_0 (as in the figure legend).

approached from the other side (negative y, polar angle $\pi < \phi < 2\pi$). Thus, insects perform the BRW as long as their position is in the upper part of the plane (i.e. for $y \geq 0$) but perform the CRW in the lower semi-plane (for $y < 0$). In order to describe the effect of bait in the upper semi-plane, we, similarly to Section 3.2, consider the attraction area where we consider R_{ATT} to be large $R_{ATT} > L$, so that insect perform the BRW in the whole upper semi-plane.

For simulations of this type, as above, we consider the circular trap of radius 5 but, in order to exclude any possible effect of domain's corners, we consider the domain of a circular shape (instead of square) of radius 50.

Fig. 11 shows snapshots of the population distribution obtained at different moments. We observe that the population distribution over space is effectively a combination of two different distribution types. The distribution in the lower semi-plane is qualitatively similar to that previously observed in case of the CRW with a sufficiently large value of parameter p_0 (cf. Fig. 4, left), with somewhat lower population density in a close vicinity of the trap compared to the rest of the domain. However, the spatial distribution in the upper semi-plane is quite different, with the population density reaching its maximum in the vicinity of the trap.

Fig. 12 shows the cumulative trap count obtained for different values of p_0. It is readily seen that, for a sufficiently large value of p_0,

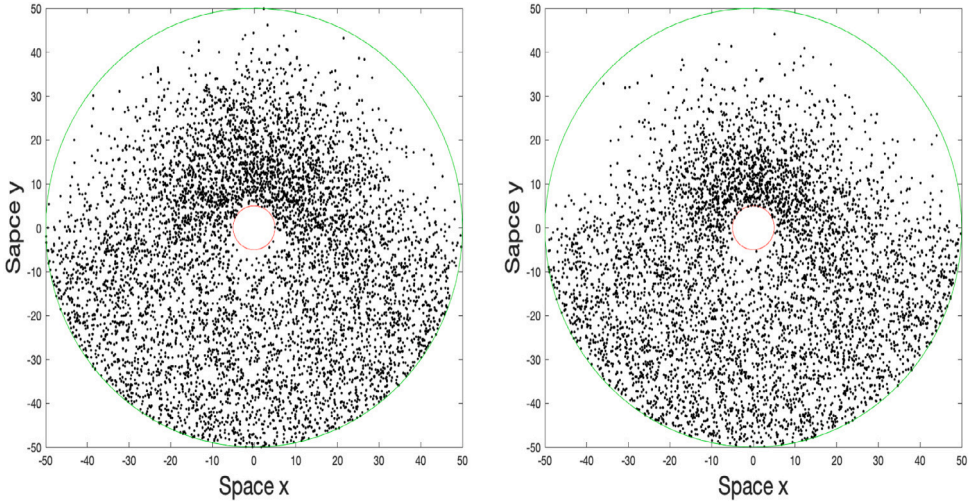

Fig. 11. Snapshots of population distribution obtained after 200 and 300 time steps (left and right, respectively) in the presence of the mixed-type trap, with the value of persistence parameter $p_0 = 2$ and $N = 8 \cdot 10^3$.

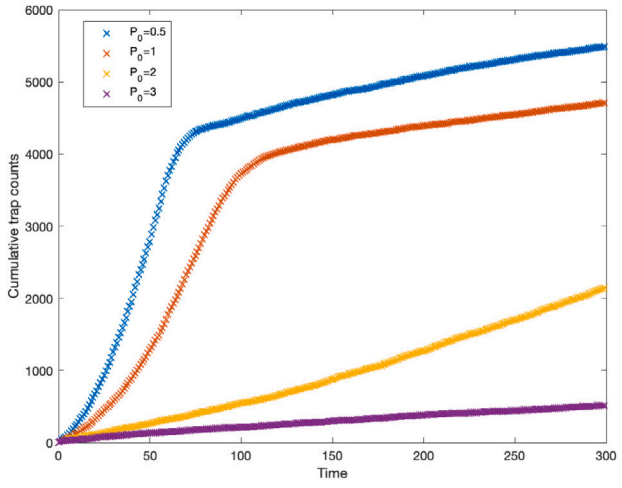

Fig. 12. Cumulative trap count obtained with a mixed-type trap for different values of the persistence parameter p_0 (as shown in the figure legend). The domain has a circular shape with radius 50, the trap radius $R = 5$, the total insect population is $N = 8 \cdot 10^3$.

the results are almost indistinguishable from those obtained in case of a baited (non-shadowed) trap. Indeed, the purple curve in Fig. 12 is practically the same as the green curve in Fig. 7, both curves being obtained for the same value $p_0 = 2$. This can be easily explained, as for large values of p_0 the BRW becomes similar to the CRW, because in both cases the turning angle is distributed almost uniformly over the circle. However, for a smaller value of p_0, some similarity only occurs at small times. For instance, the left-hand side part of the blue curve in Fig. 12 for $0 < t < 60$ has a shape similar to the corresponding part of the red curve in Fig. 7 (both being obtained for $p_0 = 0.5$), although the latter is considerably steeper. For a later time, the shape of the curves becomes rather different, an increase in the trap count being much slower in the case of the mixed-type trap.

4. Simulation results: trap counts with multiple traps

In this section, we consider how trap efficiency may be changed if another trap or traps are installed in the same domain. Each of the trap is described by its radius and the coordinates of its centre.; for instance, in case of two traps, by R_1, $\left(x^{(1)}_{trap}, y^{(1)}_{trap}\right)$ and R_2, $\left(x^{(2)}_{trap}, y^{(2)}_{trap}\right)$ for the first and second trap, respectively. All simulation settings are similar to the above, with the only difference that conditions (7)–(8) and Eq. (9) are now applied to each of the trap separately.

4.1. Combination of baited and non-baited traps

We begin with the case where there are two traps of different types placed in the domain. One of them (say, Trap 1) is non-baited, so its presence does not modify insect individual movement. Trap 2 is baited; correspondingly, in order to model the effect of bait, as well as above we introduce the attraction radius R_{ATT}. Moreover, we consider the case where the attraction radius is large, $R_{ATT} > 2L$, so that insects perform the BRW (with the bearings taken at Trap 2, cf. κ in Eq. (6)) everywhere in the domain. Each trap has the same radius, $R_1 = R_2 = 5$.

Fig. 13 shows snapshots of the population distribution obtained at a few moments of time in the case of the trap position as $\left(x^{(1)}_{trap}, y^{(1)}_{trap}\right) = (-10, -10)$ and $\left(x^{(2)}_{trap}, y^{(2)}_{trap}\right) = (25, 25)$ for non-baited and baited trap, respectively. We observe that the population distribution is strongly asymmetric, with the maximum density reached in the close vicinity of the baited trap. The non-baited trap creates a shadow, see the area of low population density at top-right of the trap. The origin of the shadow is intuitively clear. Insects walking towards baited Trap 2 from the bottom left part of the domain will never reach it, because they will be trapped by non-baited Trap 1 that they will meet on their way.

Fig. 14 shows the cumulative trap count for each of the traps. As it may be expected, except for an early time, the trap count by the baited trap (blue line) is much higher than the trap count by the non-baited trap (red line). Interestingly, the trap count by the non-baited trap appears to be somewhat larger compared to what it is in the absence of the baited trap (cf. Fig. 3). Although Trap 1 is by itself non-baited, because of its position inside the attraction (catchment) area of Trap 2, it gains extra catch by intercepting the insects travelling to Trap 2 from the bottom left corner of the domain.

4.2. Competition between two non-baited traps

In the above, we have observed that a non-baited trap introduces heterogeneity to the population spatial distribution by creating a circular shaped area in the vicinity of the trap with a significantly lower population density, this phenomenon is being the more explicit the lower the persistence is (i.e. for higher values of p_0); see Fig. 4. This is a generic effect of a non-baited trap and is seen in the mean-field model as well (Petrovskii et al., 2014, 2012). Moreover, the radius of the low density area increases with time; see Petrovskii et al. (2012) for details.

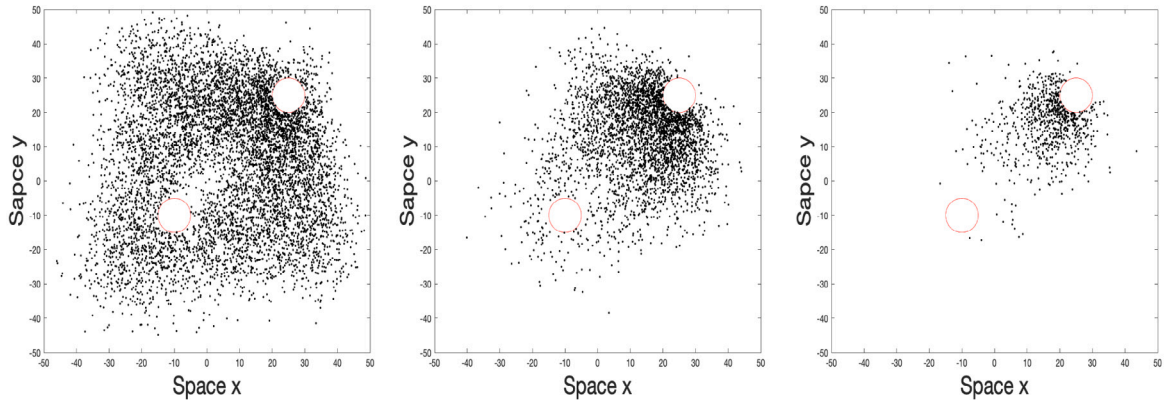

Fig. 13. Snapshots of the population distribution in the square domain with two traps (one baited, the other non-baited) obtained at time $t = 100,\ 200$ and 300, left to right, respectively. The persistence parameter is $p_0 = 1.5$.

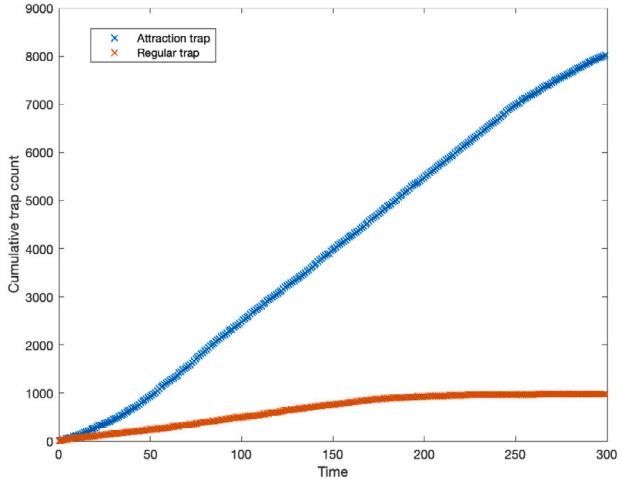

Fig. 14. Cumulative trap count vs time in the domain with two traps, blue line for the baited trap, the red line for the non-baited trap. The total insect population is $N = 10^4$, the persistence parameter is $p_0 = 1.5$.

Therefore, if more than one trap is placed in the domain, in the course of time their low density areas can start overlapping. Apparently, it can affect the trap counts for each individual trap: here we call this competition between the taps. The goal of this section is to look into this issue.

In order to make the effect of competition more explicit, we consider two different configurations. In the first configuration, we consider two non-baited traps (each of radius $R = 5$) installed far away from each other; more specifically $\left(x^{(1)}_{trap}, y^{(1)}_{trap}\right) = (-25, 0)$ and $\left(x^{(2)}_{trap}, y^{(2)}_{trap}\right) = (25, 0)$, i.e. the distance between the traps is $d_{12} = 50$. Since the growth of the low density area is known to be slow (Petrovskii et al., 2014, 2012), one can expect that any interaction between the traps in this case is negligible until after a very long time. In the second configuration, we consider the non-baited traps placed much closer to each other, namely $\left(x^{(1)}_{trap}, y^{(1)}_{trap}\right) = (0, -10)$ and $\left(x^{(2)}_{trap}, y^{(2)}_{trap}\right) = (0, 10)$, so that $d_{12} = 20$.

Fig. 15 shows the population spatial distribution obtained at different time in simulations with the first configuration. We observe that, in this case, there is no any apparent overlap between the two low density areas. On the contrary, in the second configuration (Fig. 16) the emergence of such overlap is obvious already at a relatively small time (see Fig. 16, left, obtained at $t = 1000$).

The corresponding trap counts are shown in Fig. 17. In order to reveal any possible effects of persistence, simulations were repeated for a few values of p_0, so that $p_0 = 3, 2, 1$ in Fig. 17 top to bottom, respectively. We readily observe that, expect for some early time, the cumulative trap count obtained by two traps taken together is considerably larger in the case of distant traps (the first configuration, cf. Fig. 15) than in the case of close traps (the second configuration, cf. Fig. 16). This occurs for all considered values of p_0, however the difference between the trap counts becomes larger with a decrease in p_0, i.e. when the individual animal movement becomes more directed.

The dashed line in Fig. 17 shows an estimate of the cumulative trap count obtained from the MF model (diffusion equation), as given by Eq. (10) (see Petrovskii et al., 2012 for all technical details). We therefore observe that the MF model provides a good overall description of the cumulative trap count (just slightly overestimating it for an intermediate time, e.g. approximately for $t \in (300, 1000)$ for the parameters of Fig. 17, top) in case p_0 is sufficiently large but fails when p_0 becomes small ($p_0 = 1$ or smaller). This is not surprising, in fact expected, as the individual movement is approximately diffusive (Brownian) for large values of p_0 but becomes distinctly different for a small p_0, the latter being more adequately described by the telegrapher equation rather than the diffusion equation.

4.3. Three non-baited traps

In this section, we briefly consider a somewhat more general configuration with three non-baited traps installed in the domain. All traps are of the same radius ($R = 5$) but placed at different relative position to each other, so that Trap 1 and Trap 2 are close to each other but Trap 3 is far away. Namely, the position of the traps is $\left(x^{(1)}_{trap}, y^{(1)}_{trap}\right) = (20, 10)$, $\left(x^{(2)}_{trap}, y^{(2)}_{trap}\right) = (20, -10)$ and $\left(x^{(3)}_{trap}, y^{(3)}_{trap}\right) = (-20, 0)$. Since all traps are non-baited, insects perform the CRW across the whole domain. In order to calculate the trap count, conditions (7)–(8) and Eq. (9) are applied to each of the traps.

Based on the results of Section 4.2, one can expect that the perturbation areas induced by each individual trap into the population distribution will start overlapping after a relatively short interval leaving the more distant Trap 3 unaffected for a much longer time. This is indeed what is observed in simulations. Fig. 18 shows the population distribution obtained for three moments of time. We readily observe that the low density areas around Traps 1 and 2 start overlapping already at time $t = 1000$ while there is still no any obvious overlap with Trap 3 until much later time $t = 3000$.

Since an overlap between traps tend to decrease the trap count by each of the trap, correspondingly, we expect that, except for an early time, trap counts by Traps 1 and 2 will be smaller than that by Trap 3. This is confirmed by simulations. Fig. 19 shows the cumulative trap count for each trap. At an early time, the cumulative trap count by each trap is approximately the same for all three traps. However, starting

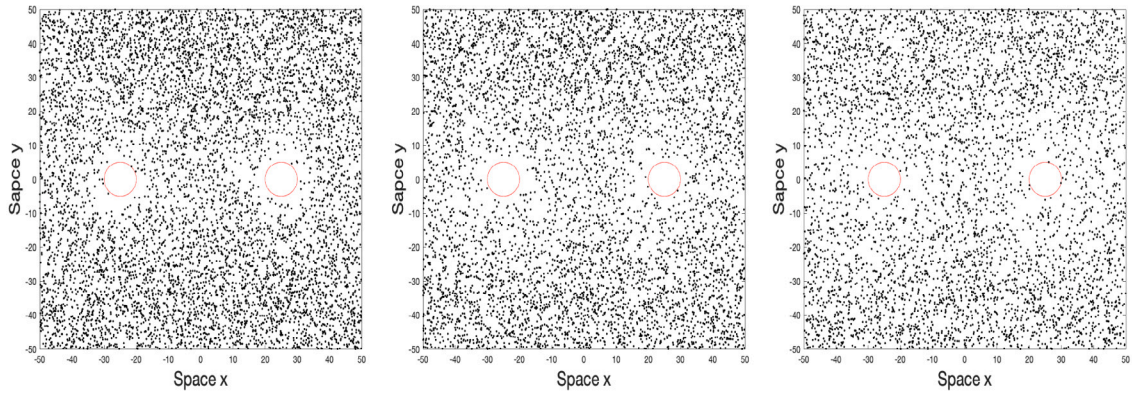

Fig. 15. Snapshots of the population distribution at a few moments of time obtained in the square domain with two non-baited traps (hence all insects performing the CRW) placed far away from each other. Left to right: $t = 1000,\ 2000,\ 3000$. The total insect population is $N = 10^4$ and the persistence parameter is $p_0 = 2$.

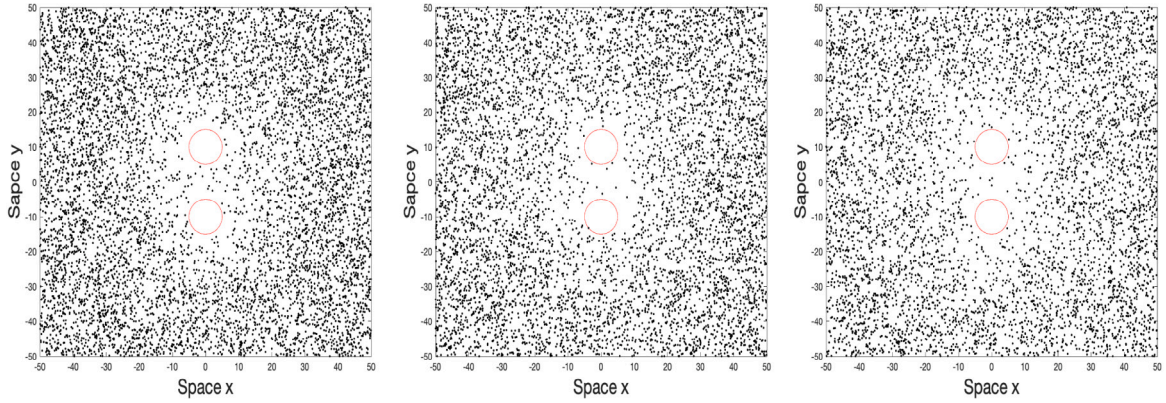

Fig. 16. Snapshots of the population distribution at a few moments of time obtained in the square domain with two non-baited traps placed close to each other. Left to right: $t = 1000,\ 2000,\ 3000$. The total insect population is $N = 10^4$ and the persistence parameter is $p_0 = 2$.

from approximately $t = 100$ Trap 3 has a higher cumulative trap count. Note that the trap counts by Traps 1 and 2 coincide at all time, as these two traps are perfectly identical.

5. Discussion and conclusions

Traps are commonly used in insect ecology and pest control (Epsky et al., 2008; Pedigo, 1999) for at least two different reasons. Firstly, trap counts provide information about the presence (and sometimes abundance) of a given species in the vicinity of the trap (Baars, 1979; Raworth and Choi, 2001; Johnson, 1969). Secondly, traps, especially baited traps (such as, depending on the species traits, pheromone baited, light baited, colour baited, etc.) are used for mass trapping, i.e. to catch and kill/remove insects in large numbers as a part of pest management (El-Sayed et al., 2006). In spite of this, neither the factors affecting the trap count nor the extent of the disturbance that the trap can introduce into the population distribution are well understood. This is particularly true in case of baited traps, because their effect changes the movement behaviour (e.g. by turning isotropic random movement into more directed movement towards the trap) and hence is much more complicated than that of non-baited traps.

In this paper, by using numerical simulations of individual insect movement of different type (cf. CRW and BRW, see Section 2.2), we have provided a systematic investigation into the dynamics of animal trapping by traps of various design (such as non-baited, baited and hybrid). We considered both the issue of the trap efficiency, i.e. how fast the cumulative trap count may increase over time, and the effect that the trap may exert onto the spatial population distribution in the domain where the trap is installed. Our main findings are summarised below:

1. Both for a non-baited and baited traps, the cumulative trap count essentially depends on the persistence of animal individual movement, i.e. on the variance of the turning angle distribution (cf. parameter p_0 in Eqs. (5) and (6), respectively). The smaller the variance, the larger the trap count is; see Figs. 3 and 10. This is in agreement with intuitive expectations. Indeed, in case of a small p_0 (high persistence), the movement path becomes close to a straight line and the movement pattern becomes close to ballistic. Correspondingly, over a given time interval, the number of animals that can be trapped is higher as they may travel to the trap from locations further away. Hence, the 'catchment area' of the trap is larger than in the case of large p_0 (low persistence). Essentially, this is a result of the obvious observation that the ballistic movement is faster than the diffusive one (Codling et al., 2008; Turchin, 1998; Viswanathan et al., 2011).
2. A baited trap is not at any time equivalent to a large non-baited trap (where the radius for the latter is defined as the radius of the attraction area of the former); see Section 3.2. At an early time, the large non-baited trap has a higher cumulative trap count than the baited one but this change to the opposite in the course of time (see Fig. 5).
3. In case where there are more than one trap installed in the domain, their efficiency tends to decrease with time: as their growing catchment areas may start overlapping in the course of time, the traps start 'competing' between themselves. This effect is seen clearer when traps are installed close to each other; see Fig. 19.
4. For a non-baited trap, the mean-field approximation (10) derived from the diffusion equation (see Petrovskii et al. (2012) for

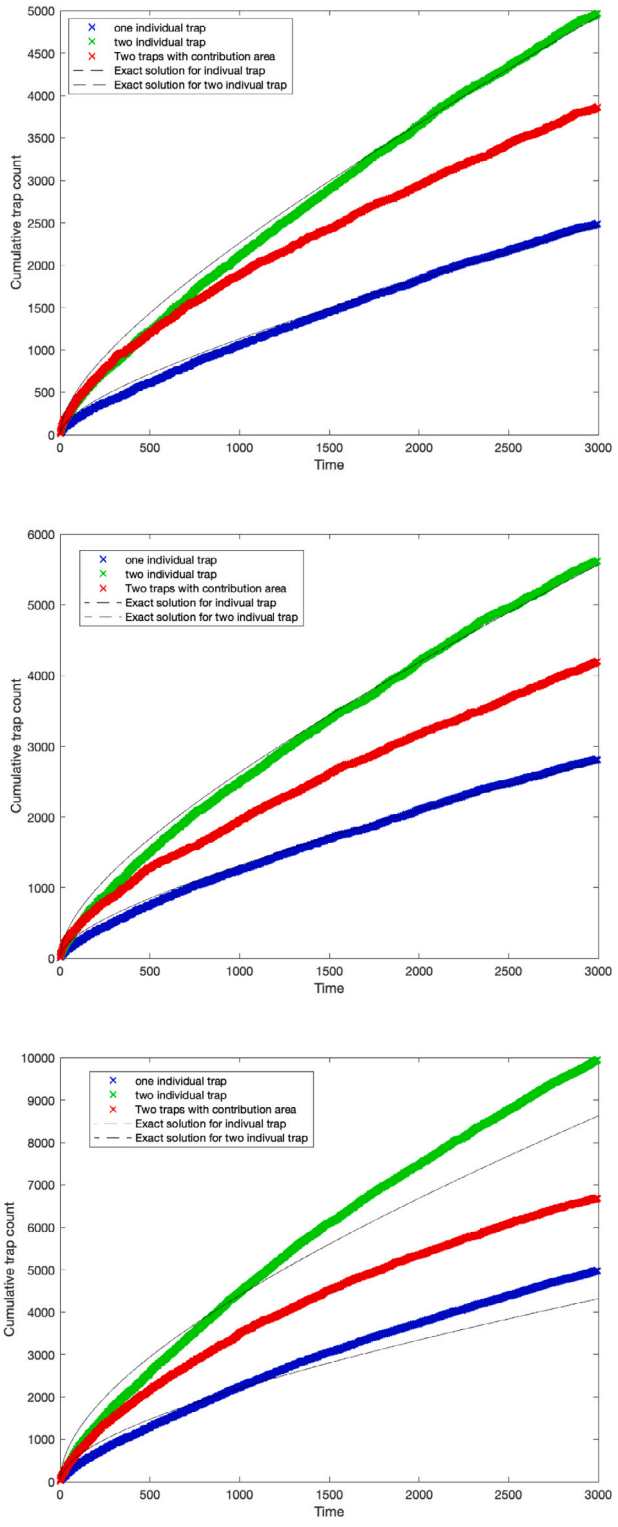

Fig. 17. Cumulative trap counts obtained in the two trap case for the two configurations: green curve for the traps placed far away from each other, red curve for the traps paced close to each other. Panels top to bottom correspond to different values of the persistence parameter, $p_0 = 3, 2$ and 1, respectively. As a reference case, the blue line shows the cumulative trap count obtained for a single trap. The dashed line shows the mean-field approximation using Eq. (10).

details) provides reasonably good overall description of the cumulative trap count in case of low-persistence individual movement $p_0 \geq 2$ but clearly fails in case of high-persistence movement $p_0 \leq 1$ (see Fig. 17). The failure is readily explained by the fact that the population dynamics in case of high-persistence movement is more adequately described by a different MF model (e.g. the telegrapher equation) instead of the diffusion equation (Alharbi and Petrovskii, 2018; Tilles and Petrovskii, 2019; Holmes et al., 1994).

5. Trap introduces heterogeneity in the spatial population distribution and can even lead to the pattern formation. In case of a non-baited trap, such emerging heterogeneity is an area around the trap where the population density falls to a small value compared to the rest of the domain. The effect of a baited trap can, depending on the domain shape, result in a stronger heterogeneity by creating a curiously shaped pattern of high population density (cf. Fig. 8). In the case where two traps of different types are installed, their interaction can lead to the formation of a shadow in the vicinity of the non-baited trap (Fig. 13).

We emphasise that all our results are essentially new. Although there is plenty of modelling studies addressing various aspects of individual animal movement (e.g. Turchin, 1998; Jopp and Reuter, 2005; Viswanathan et al., 2011; Pyke, 2015), this is usually done in the context of migration, foraging and/or search efficiency. There is only a small number of papers where animal movement is modelled in relation to trapping. Current understanding of the factors affecting trap counts collected by a baited trap, as well as trap's possible feedback onto the spatial distribution of the monitored/controlled population, is at its infancy and almost entirely lacking the required rigour. Here we have shown for the first time that the intuitive concept of the trap catchment area (or the effective sampling area) often used for the interpretation of the trap counts by a baited trap can be grossly misleading (see Item 2 above). We have also shown for the first time that a baited trap can bring a significant disturbance to the spatial population distribution on the field scale (cf. Item 5). This new result may have a variety of important implications for modelling agri-ecological systems where trapping is often a standard part of the agricultural procedures.

Since the IBM framework that we used in our study is inherently stochastic, a question may arise as to what extent our results are representative and reproducible. Indeed, in a generic stochastic system, a single realisation (e.g. a simulation run) is hardly informative, i.e. at best showing what may happen but not telling anything how likely that happens. (In the context of animal movement, that applies to animal's movement path, as every new simulation run produces a different trajectory.) However, the *averaging* of the results over multiple realisations gives an estimate of the mean, which is a stable and reproducible quantity. Moreover, by the virtue of the Central Limit Theorem, the variance of the deviations from the mean is known to decrease with the number of realisations. In our study, the trap count emerges as a contribution from many individual animals with identical properties. Although trapping of each individual animals is an entirely random event, the contribution from many such events acts as averaging: it was shown in earlier studies (Petrovskii et al., 2014, 2012) that deviations from the cumulative trap count becomes negligibly small when the number of animals is sufficiently large. In a system with a small number of animals, similar regularisation is achieved by averaging over several stochastic realisations (Petrovskii et al., 2014, 2012).

Our study leaves a few open questions. Perhaps the main one is the possible effect of the heterogeneity of animal movement behaviour. Such heterogeneity may arise through a variety of reasons. One reason is the individual differences that are inherent in any species. In terms of our approach, the presence of individual differences means that the parameters of individual movement (cf. p_0 and δ) can be different for different animals. The population as a whole is then described

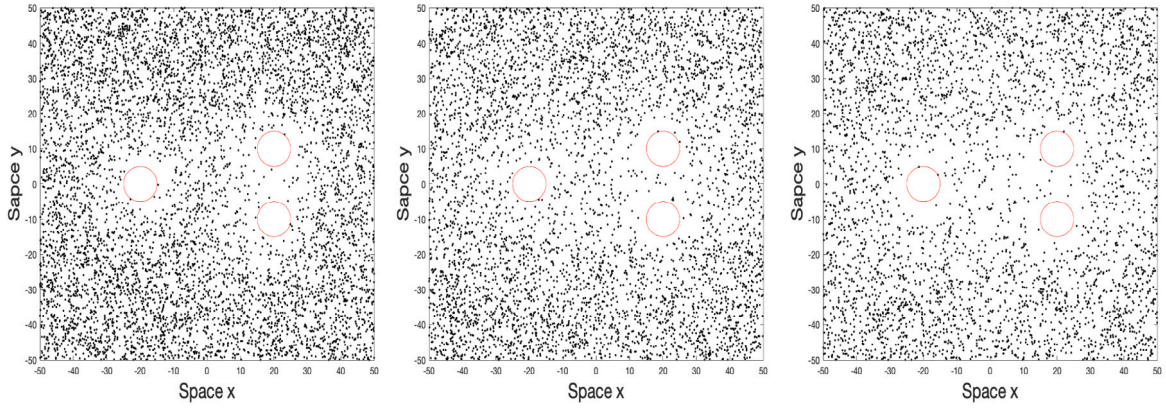

Fig. 18. Snapshots of the spatial population distribution simulated in a square domain with three non-baited traps installed. Animals perform the CRW with the persistence parameter $p_0 = 2$. Left to right: $t = 1000$, $t = 2000$, $t = 3000$.

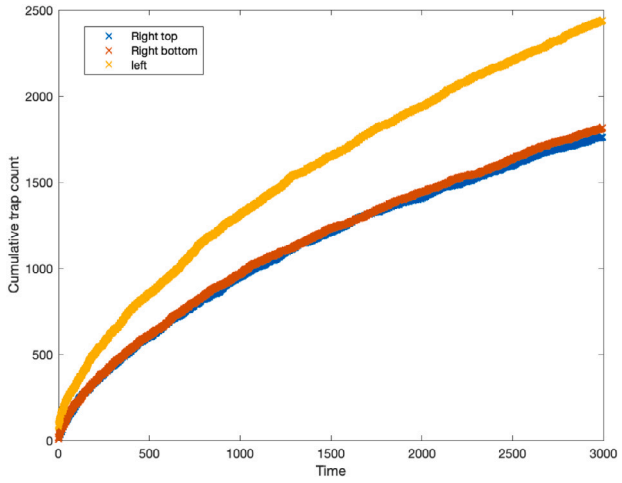

Fig. 19. Cumulative trap count for the configuration with three traps. Here the blue and red curves are for Traps 1 and 2 that are close to each other and the yellow curve is for Trap 3 that is placed much farther away (see details in the text). Persistence parameter is $p_0 = 2$. The total initial population size is 10^4.

not by a given parameter value but by a distribution of different value's frequency. Depending on the properties of the distribution, the resulting effect on the trap counts can be considerable (Petrovskii et al., 2014).

Another source of heterogeneity is the differential animal response to the trap's attracting agent, i.e. the bait. In the present study, we assumed that the agent acts on the animal movement behaviour uniformly in space: as soon as animal's position is within the attraction radius, its movement becomes more ordered, i.e. more directed towards the trap. However, this is of course a caricature of reality. It is more likely that the strength of the attracting agent decreases continuously with the distance from the trap and hence any possible change in the animal movement behaviour occurs gradually rather than abruptly. Understanding of the effects of this additional spatial heterogeneity lies beyond the scope of this paper but will become the focus of future work.

Declaration of competing interest

The authors declare that they have no known competing financial interests or personal relationships that could have appeared to influence the work reported in this paper.

Acknowledgements

This work was supported by EPSRC, UK through Project EP/T027371/1 (to S.P.). O.A. was supported by the Saudi Embassy in the form of a full PhD scholarship. Also, he is very grateful to the University of Leicester for the academic support.

References

Ahmed, D.A., Petrovskii, S.V., 2019. Analysing the impact of trap shape and movement behaviour of ground-dwelling arthropods on trap efficiency. Methods Ecol. Evol. 10 (8), 1246–1264.
Alharbi, W., Petrovskii, S., 2018. Critical domain problem for the reaction-telegraph equation model of population dynamics. Mathematics 6, 59.
Baars, M., 1979. Catches in pitfall traps in relation to mean densities of carabid beetles. Oecologia 41 (1), 25–46.
Bearup, D., Benefer, C., Petrovskii, S., Blackshaw, R., 2016. Revisiting Brownian motion as a description of animal movement: a comparison to experimental movement data. Methods Ecol. Evol. 7, 1525–1537.
Bearup, D., Petrovskaya, N., Petrovskii, S., 2015. Some analytical and numerical approaches to understanding trap counts resulting from pest insect immigration. Math. Biosci. 263, 143–160.
Binns, M.R., Nyrop, J.P., van der Werf, W., Werf, W., 2000. Sampling and Monitoring in Crop Protection: The Theoretical Basis for Developing Practical Decision Guides. Cabi.
Boetzl, F.A., Ries, E., Schneider, G., Krauss, J., 2018. It'sa matter of design—how pitfall trap design affects trap samples and possible predictions. PeerJ 6, e5078.
Brown, G.R., Matthews, I.M., 2016. A review of extensive variation in the design of pitfall traps and a proposal for a standard pitfall trap design for monitoring ground-active arthropod biodiversity. Ecol. Evol. 6 (12), 3953–3964.
Bullock, J., Kenward, R., Hails, R., 2002. Dispersal Ecology. Blackwell.
Byers, J.A., 1999. Effects of attraction radius and flight paths on catch of scolytid beetles dispersing outward through rings of pheromone traps. J. Chem. Ecol. 25 (5), 985–1005.
Byers, J.A., Anderbrant, O., Löqvist, J., 1989. Effective attraction radius. J. Chem. Ecol. 15 (2), 749–765.
Clobert, J., Danchin, E., Dhondt, A., Nichols, J., 2001. Dispersal. Oxford University Press.
Codling, E.A., Plank, M.J., Benhamou, S., 2008. Random walk models in biology. J. R. Soc. Interface 5 (25), 813–834.
Edelhoff, H., Johannes Signer, J., Balkenhol, N., 2016. Path segmentation for beginners: An overview of current methods for detecting changes in animal movement patterns. Mov. Ecol. 4, 21.
El-Sayed, A., Suckling, D., Wearing, C., Byers, J., 2006. Potential of mass trapping for long-term pest management and eradication of invasive species. J. Econ. Entomol. 99 (5), 1550–1564.
Engel, J., Hertzog, L., Tiede, J., Wagg, C., Ebeling, A., Briesen, H., Weisser, W.W., 2017. Pitfall trap sampling bias depends on body mass, temperature, and trap number: insights from an individual-based model. Ecosphere 8 (4), e01790.
Epsky, N.D., Morrill, W.L., Mankin, R.W., 2008. Traps for capturing insects. Encycl. Entomol. 3, 2318–2329.
Guichard, S., Kriticos, D., Leriche, A., Kean, J., Worner, S., 2012. Individual-based modelling of moth dispersal to improve biosecurity incursion response. J. Appl. Ecol. 49, 287–296.
Holmes, E.E., Lewis, M.A., Banks, J., Veit, R., 1994. Partial differential equations in ecology: spatial interactions and population dynamics. Ecology 75 (1), 17–29.

Johnson, C.G., 1969. Mechanisms of Insect Dispersal: Migration and Dispersal of Insects by Flight. Methuen & Co. Ltd., London.
Jonason, D., Franzén, M., Ranius, T., 2014. Surveying moths using light traps: effects of weather and time of year. PLoS One 9 (3), e92453.
Jopp, F., Reuter, H., 2005. Dispersal of carabid beetles - emergence of distribution patterns. Ecol. Model. 186, 389–405.
Kareiva, P., Shigesada, N., 1983. Analyzing insect movement as a correlated random walk. Oecologia 56 (2–3), 234–238.
Klafter, J., Shlesinger, M.F., Zumofen, G., 1996. Beyond Brownian motion. Phys. Today 49 (2), 33–39.
McDonald, J., Hodgson, D., 2021. Counting cats: The integration of expert and citizen science data for unbiased inference of population abundance. Ecol. Evol. 11, 4325–4338.
Pedigo, L.P., 1999. Entomology and Pest Management, third ed. Prentice Hall, Upper Saddle River.
Petrovskii, S., Bearup, D., Ahmed, D.A., Blackshaw, R., 2012. Estimating insect population density from trap counts. Ecol. Complex. 10, 69–82.
Petrovskii, S., Ellis, J., Forbes, E., Petrovskaya, N., Walters, K.F., 2022. A predictive model and a field study on heterogeneous slug distribution in arable fields arising from density dependent movement. Sci. Rep. 12 (1), 1–12.
Petrovskii, S., Petrovskaya, N., Bearup, D., 2014. Multiscale approach to pest insect monitoring: random walks, pattern formation, synchronization, and networks. Phys. Life Rev. 11 (3), 467–525.
Pyke, G.H., 2015. Understanding movements of organisms: it's time to abandon the Lévy foraging hypothesis. Methods Ecol. Evol. 6 (1), 1–16.
Raworth, D.A., Choi, M.-Y., 2001. Determining numbers of active carabid beetles per unit area from pitfall-trap data. Entomol. Exp. Appl. 98 (1), 95–108.
Seber, G.A.F., 1982. The Estimation of Animal Abundance and Related Parameters. Blackburn Press Caldwell, New Jersey.
Tilles, P., Petrovskii, S., 2019. On the consistency of the reaction-telegraph process within finite domains. J. Stat. Phys. 177, 569–587.
Tonnanga, H., et al., 2017. Advances in crop insect modelling methods - Towards a whole system approach. Ecol. Model. 354, 88–103.
Turchin, P., 1998. Quantitative Analysis of Movement. Sinauer.
Turchin, P., 2013. Complex Population Dynamics. Princeton University Press.
Turchin, P., Odendaal, F., 1996. Measuring the effective sampling area of a pheromone trap for monitoring population density of southern pine beetle (Coleoptera: Scolytidae). Environ. Entomol. 25, 582–588.
Viswanathan, G.M., Afanasyev, V., Buldyrev, S.V., Murphy, E.J., Prince, P.A., Stanley, H.E., 1996. Lévy flight search patterns of wandering albatrosses. Nature 381 (6581), 413–415.
Viswanathan, G.M., Da Luz, M.G., Raposo, E.P., Stanley, H.E., 2011. The physics of foraging: an introduction to random searches and biological encounters. Cambridge University Press.
Yamanaka, T., Tatsuki, S., Shimada, M., 2003. An individual-based model for sex-pheromone-oriented flight patterns of male moths in a local area. Ecol. Model. 161, 35–51.